Title	Beam Current Monitor with a Troidal Coil for a Pulsed Proton Beam
Author(s)	Dewa, Hideki; Iwashita, Yoshihisa; Fujita, Hirokazu; Ikegami, Masanori; Inoue, Makoto; Kakigi, Shigeru; Kando, Masaki; Noda, Akira; Okamoto, Hiromi; Shirai, Toshiyuki
Citation	Bulletin of the Institute for Chemical Research, Kyoto University (1994), 72(1): 76-86
Issue Date	1994-03-31
URL	http://hdl.handle.net/2433/77546
Right	
Type	Departmental Bulletin Paper
Textversion	publisher

Beam Current Monitor with a Troidal Coil
for a Pulsed Proton Beam

Hideki DEWA*, Yoshihisa IWASHITA*, Hirokazu FUJITA*, Masanori IKEGAMI*,
Makoto INOUE*, Shigeru KAKIGI*, Masaki KANDO*, Akira NODA*,
Hiromi OKAMOTO* and Toshiyuki SHIRAI*

We developed a pulsed beam current monitor with a troidal coil. A new current-to-voltage converter enabled a measurement of a pulsed beam with the pulse width of 50 μs without deformation of the pulsed signal. From 30 μA to 10 mA, wide range beam current can be measured. The pickup coil is sealed in a glass container for the easy production and the vacuum isolation. We could successfully measure the pulsed proton beam at a peak current of 250 μA, and a pulse width of 50 μs.

KEY WORDS: Beam Current / Pulsed Beam / Beam Monitor / Current Transformer / Current Monitor / Troidal Core / Negative Impedance Converter

1. INTRODUCTION

For the pulsed current measurement of a charged particle beam, the current monitor with a troidal coil has a disadvantage of the drooped pulse shape[1],[2],[3],[4]. The finite inductance of the troidal coil and the non-zero input impedance of the current-to-voltage converter cause this droop.

The pulse width of our ICR proton linac is around 50 μs, and the minimum peak current to be measured is the order of 100 μA. For the measurement by the oscilloscope, the conversion gain must be greater than 1000 V/A, and the time constant of the droop must be longer than 1 ms.

A resistor is the simplest current-to-voltage converter as shown in Fig. 1 (a), but the resistance should be determined carefully. Higher resistance is needed for getting a high output voltage, and the lower resistance is needed for the less droop.

A conventional circuit with an operational amplifier for the current-to-voltage converter is shown in Fig. 1 (b). When this circuit is used as the converter, the DC level of the input is grounded by the coil and this circuit does not operate properly. We developed a new converter circuit with low input impedance and high gain.

2. PICKUP COIL

The beam current monitor using a troidal coil is a current transformer as shown in Fig.

*出羽英紀、岩下芳久、冨士田浩一、池上雅紀、井上　信、柿木　茂、神門正城、野田　章、岡本宏巳、
白井敏之 : Nuclear Science Research Facility, Institute for Chemical Research, Kyoto University.
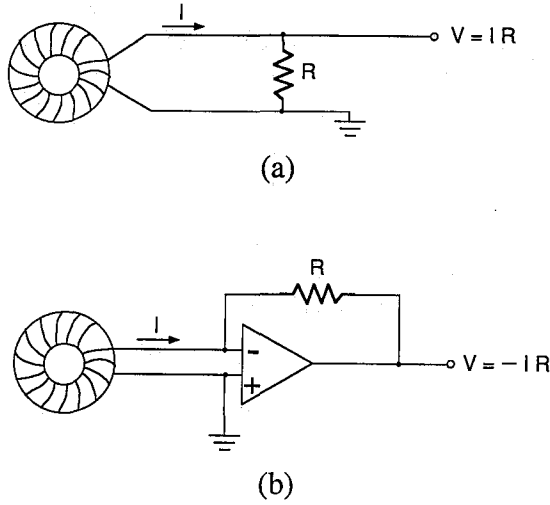
(a)

(b)

Fig. 1 Schematic diagram of the conventional current-to-voltage converter. (a) A re-
sistor is the current-to-voltage converter. (b) A conventional circuit of the
current-to-voltage converter by an operational amplifier.

2. When the charged particle beam passes through the troidal core, the secondary current is
induced. The induced current I_2 is given by

$$I_2 (t) = \frac{I_1}{n} \exp \left(-\frac{Z}{L} t \right), \qquad (1)$$

where I_1, n, Z, and L are the pulsed beam current, the number of turns of the secondary wind-
ing, the inductance of the coil, and the input impedance of the corrent-to-voltage converter, re-
spectively. From this relation, more secondary current can be obtained by fewer turns of
secondary winding. On the other hand, the droop of the pulse shape is expressed by the ex-
ponential term of the equation (1). Because L/Z is the time constant of the droop, lower Z and
higher L are desirable for the small droop.

The frequency characteristics of the current monitor with a troidal coil depend on the
magnetic characteristic of the core, the inductance of the pickup coil, and the input impedance
of the current-to-voltage converter. Because the rise time of the pulsed beam is the order of 1
μs, the core must have enough frequency characteristics. Amorphous or ferrite core is
appropriate to this purpose. The inductance of the coil is given by

$$L = A_L \times n^2 \quad [nH], \qquad (2)$$

where A_L is the constant of the core and depends on the magnetic permeability and the shape
of the core. A_L is given by

$$A_L = \frac{4\pi \mu S}{\ell_m} \quad [nH/n^2], \qquad (3)$$

where μ is the relative magnetic permeability, ℓ_m [cm] is the magnetic circuit length, and S
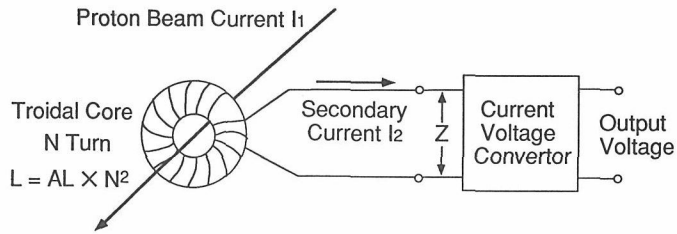
Fig. 2 Schematic diagram of the pulsed beam measurement.

$[cm^2]$ is the cross section of the core. For less droop, larger n is desirable, but the secondary output current becomes low.

The pickup coil is shown in Photo 1. The core of the current transformer is made of ferrite, which is TDK H5C2 T28×13×16. The relative magnetic permeability of the troidal core is 10000, the inner and outer diameters are 13 mm and 28 mm respectively, and the width is 16 mm. The A_L of the core is 14000 nH/n^2, and the number of the turns is 30. The calculated inductance of the coil is 12.6 mH. Considering the easiness of the production and the vacuum isolation, it is sealed in a glass container whose inner and outer diameter is 10 mm and 40 mm respectively. The secondary winding is a copper wire coated by a formal resin. The diameter of the wire is 0.5 mm, which is covered with a glass fiber tube for insulation considering a hot environment in the sealing process.

3. CURRENT-TO-VOLTAGE CONVERTER

If a resistor is used as a current-to-voltage converter, its resistance R is just the input impedance Z. Because the output voltage is given by

$$V(t) = RI_2 = \frac{RI_1}{n} \exp\left(-\frac{R}{L}t\right),\tag{4}$$

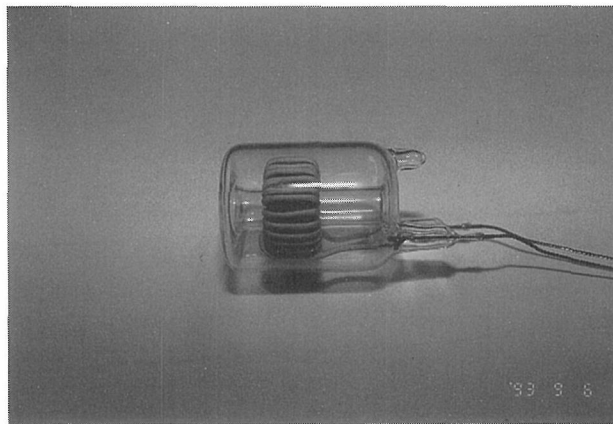a high output voltage and a small droop are not compatible.

Photo 1 Pickup coil sealed in a glass container.

Because a current-to-voltage converter with high gain and low input impedance was the requirement, we developed a new converter circuit with an operational amplifier. A schematic circuit diagram of the current-to-voltage converter is shown in Fig. 3. This circuit is an application of the Negative Impedance Converter[5),6)] (NIC). The ratio of the input current I_a and the inverse current I_b is given by

$$\frac{I_a}{I_b} = \frac{R_3}{R_2}.$$ (5)

Because the directions of the current I_a and I_b are opposite, this circuit acts as the current inverter. The input impedance of this circuit is given by

$$Z = \frac{R_1 R_3 - R_2 R_4}{R_3}.$$ (6)

Therefore, when the following condition is satisfied;

$$R_1 R_3 = R_2 R_4 ,$$ (7)

the input impedance becomes zero, and the time constant of the droop L/R becomes theoretically infinite. The output voltage is given by

$$V = -R_4 I_b = -R_1 I_a .$$ (8)

The conversion gain of the current-to-voltage converter is $-R_1$ $[\Omega]$.

The detailed circuit diagram of the designed current-to-voltage converter is shown in Fig. 4. To keep the equation (7), precision metal-film resistors are used as these four resistors, and R_1 is composed of a metal-film resistor and a variable resistor. The variable resistor should be adjusted as the droop of the wave form is decreased. Because the resistor R_3 is low, the large output current increases the power dissipation in the amplifier, and raises its temperature. Therefore a current booster circuit is attached at the output of operational amplifier,
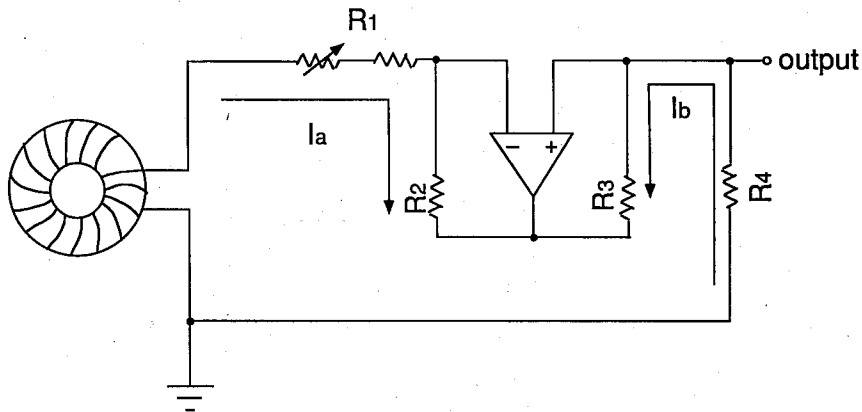

Fig. 3 Schematic circuit diagram of the current-to-voltage converter. This circuit is an application of the negative impedance converter.

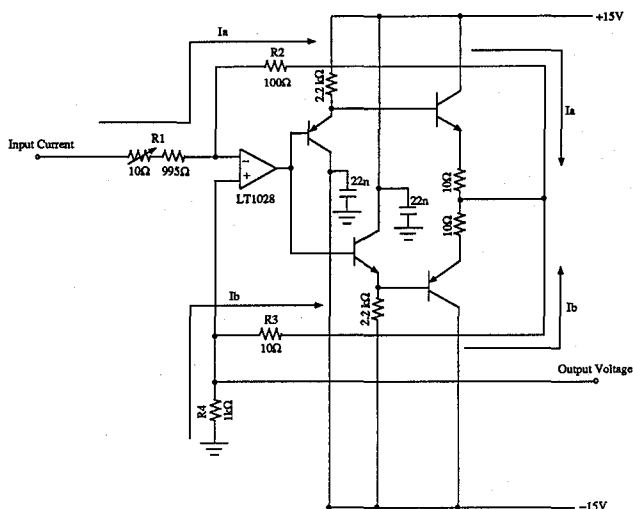H. DEWA, Y. IWASHITA, H. FUJITA, M. IKEGAMI, M. INOUE, S. KAKIGI, M. KANDO

Fig. 4 Detailed circuit diagram of the current-to-voltage converter. The operational
amplifier and the four resistors R1~ R4 are the main parts of the converter. A
current booster circuit is connected to the output of the operational amplifier.

that can decrease the thermal drift of the operational amplifier.

4. PERFORMANCE TEST BY THE TEST CURRENT

The current monitor was tested with a function generator. The schematic block diagram
of the measurement setup is shown in Fig. 5. The test pulse current of 10 μA was fed to the
primary winding of one.turn. The output of the current monitor is shown in Fig. 6 (a). Be-
cause the noise level of about 30 mV is higher than the signal of 10 mV, the pulse shape is not
clear. Thus the minimum current that can be measured is about 30 μA. When the primary
current was 1 mA, the rise time of the pulse was 1 μs as shown in Fig. 6 (b). The rise time is
enough for the measurement of our proton beam. The output signals at the primary currents
of 100 μA and 10 mA are shown in Fig. 6 (c) and 6 (d) respectively. We could measure the
test pulsed current without droop precisely.

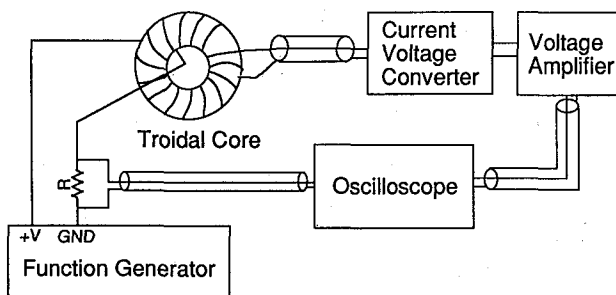The input impedance of the converter should be adjusted to zero by the variable resistor

Fig. 5 Setup for the measurement of the test current.
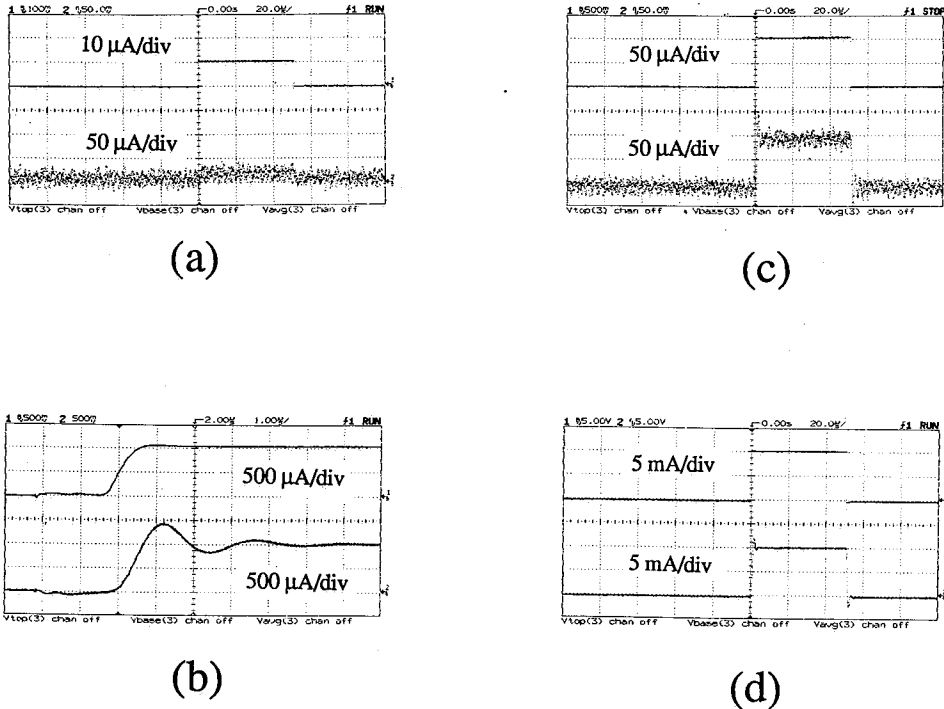
(a)

(c)

(b)

(d)

Fig. 6 Output signals of the circuit tests. The top signals are from the function gener-
ator. The bottom signals are from the current monitor, whose conversion gain
is 1 mA/1 V. (a) The primary current is 10 μA. The time scale is 20 μs/div.
(b) The primary current is 1 mA. The time scale is 1 μs/div. (c) The primary
current is 100 μA. The time scale is 20 μs/div. (d) The primary current is
10 mA. The time scale is 20 μs/div.

so that the droop of the pulse shape decreases. The output pulse shape before and after the
adjustment are shown in Fig. 7. The droop in the 50 μs pulse is evaluated as 0.2% from the
droop with the pulse width of 8 ms. The linearity of this monitor was verified within 5% from
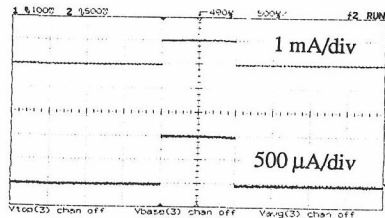30 μA to 10 mA of the primary current.

5. MEASUREMENT SETUP

The beam current was measured at the beam matching section between RFQ linac and
Alvarez linac. The current monitor was installed in the holder for the permanent magnetic
quadrupoles (PMQ) as shown in photo 2. The schematic view of the beam matching section is
shown in Fig. 8. The current of the proton beam was measured at two positions, one is after
the RFQ linac, and the other is just before the Alvarez linac.

The block diagram of the current monitor is shown in Fig. 9. The secondary current goes
through the coaxial cable and feed through, to the current-to-voltage converter. Because the
number of turns of the coil is 30, the gain of second stage is decided as 30, and thus the total
conversion gain of the current-to-voltage converter is 1000. Then the output signal goes to the
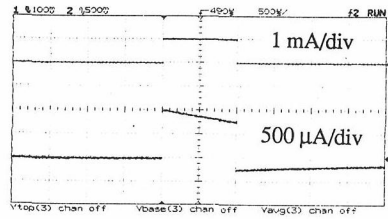
(a)

(b)

Fig. 7 The adjustment of the variable resistor. The top signals show the input current generated by the function generator, and the bottom signals are the outputs of the current monitor. The primary current is 1 mA. The time scale is 500 μs/div. (a) Before adjusting the variable resistor. There is a droop in the output of the current monitor. (b) After adjusting the variable resistor. The droop is not seen in the 1 ms width.
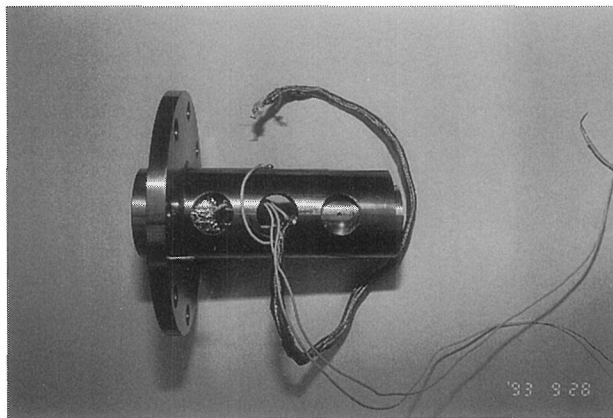

Photo 2 Pickup coil in the PMQ holder. This PMQ holder is set on the end plate of the Alvarez linac. Two PMQs are set on the right hand side (up stream), and the pickup coil is set on left hand side (down stream).

offset canceling circuit in the control room that is located out of the accelerator room, and the processed signal is measured by the oscilloscope.
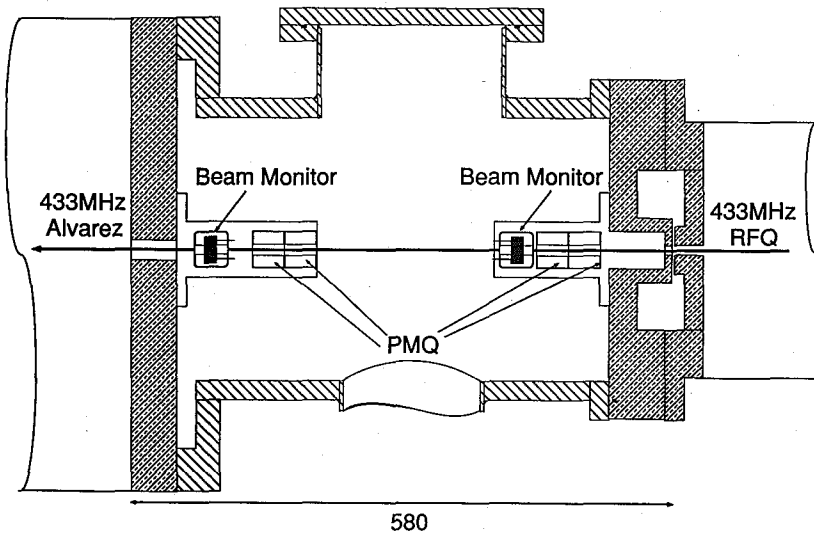
Fig. 8 Schematic view of the beam matching section. The proton beams are acceler-
ated to 2 MeV by the 433 MHz RFQ linac. Through the beam matching section,
the proton beams are accelerated to 7 MeV by the 433 MHz Alvarez linac. The
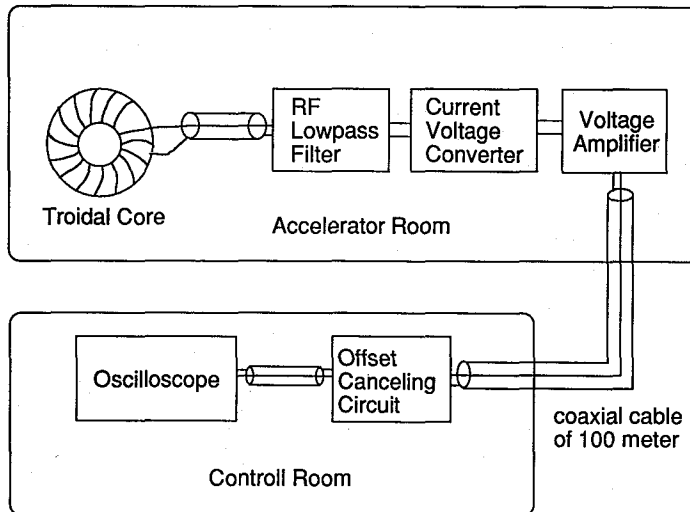transverse beam matching is performed by the permanent magnetic quadru-
poles.

Fig. 9 Block diagram of the current monitor.

Because the coil is installed between the RFQ linac and the Alvarez linac which keep
high power RF of 433 MHz in them, even small fraction of the power leak can be picked up by
the coil. To eliminate the RF contamination, a low pass filter with 200 MHz cutoff is inserted
between the coil and the converter. The low pass filter was directly connected to the BNC

(83)

feed through, so that the distanse between the coil and the converter was made as short as possible.

There are two reasons that cause the offset of the output signal. One is the thermal drift of the operational amplifier, and the other is the hum from the commercial power line (60 Hz). Decreasing the power supply voltage of the operational amplifier of the current-to-voltage converter, and adding the current booster reduce the thermal drift. It was not easy to suppress the hum noise. Because the current converter is also sensitive to the low frequency signal, the level of the hum is comparable to the real beam signal at the small beam current. Although the aluminum thin foil is wrapped around the glass container as the electric shield, it is not effective to such low frequency noise. Preliminary test indicates that the magnetic shield by a material of high magnetic permeability such as permalloy is effective. There is a plan to put the magnet shield around the core.

To keep the offset level at zero, we added the offset canceling circuit after the converter. The diagram of this circuit is shown in Fig. 10 (a). This circuit holds the output level of the converter just before the pulse, and subtracts this level from the original input signal as shown in Fig. 10 (b). The timing of the sample hold is given by the timing generator of the accelerator system.
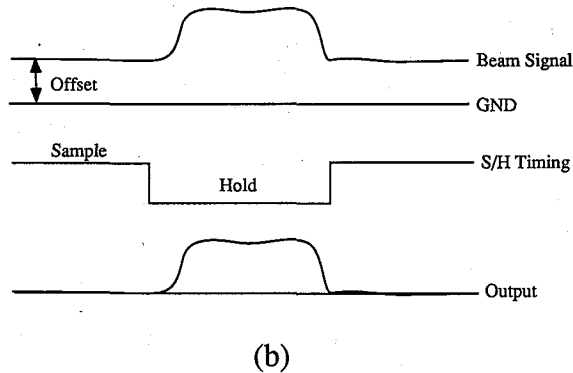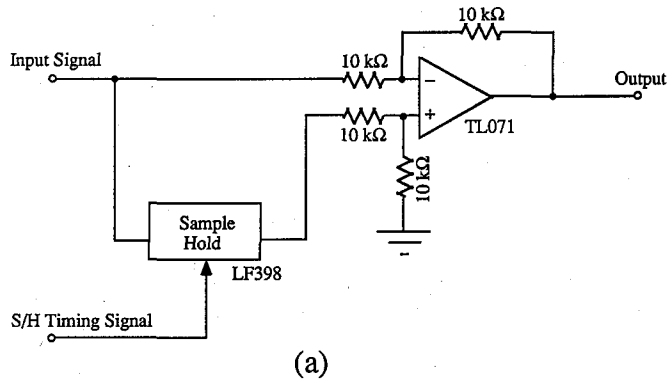
Fig. 10 (a) Schematic circuit diagram of the offset canceling circuit.
(b) Function of the offset canceling circuit.

The offset canceling circuit was examined with the test current fed from the function generator. The offset in the output of the current-to-voltage converter is shown in bottom signal of Fig. 11. The slow fluctuations caused by the thermal drift of the operational amplifier and the fast flutter caused by the hum are superimposed. The top signal is an output from the offset canceling circuit connected after the voltage amplifier. It shows that the offset was canceled. Because the hum contamination observed in the acceleration room was larger than that in this test measurement, this offset canceling circuit was necessary for the beam measurement.

6. BEAM MEASUREMENT

The measured beam current after the RFQ linac is shown in the top of the photo 3 and that before the Alvarez linac is shown in the bottom. Two dips were observed just before and after the beam pulse in the top signal. Because these dips were not observed by the second monitor, this signal is thought to be induced by the electrons from the RFQ. The measured
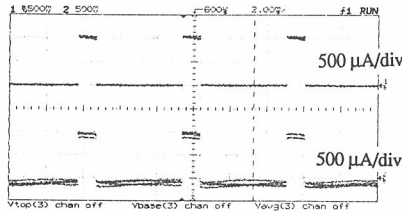

Fig. 11 The low frequency noise in measuring the test pulsed current. The bottom signal is the output of the current-to-voltage converter. The top signal is the output of the offset canceling circuit. The primary current is 1 mA. The time scale is 2 ms/div.
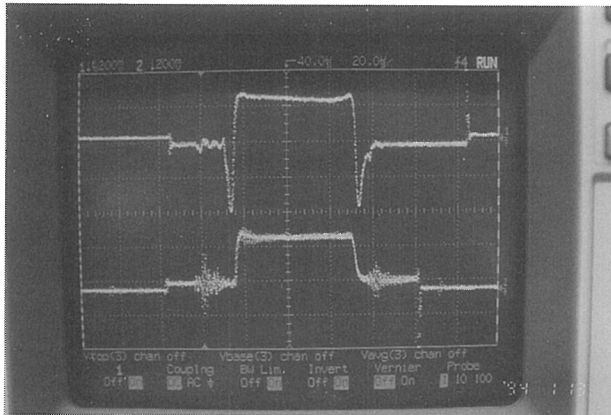

Photo 3 Pulsed beam current measured in the beam matching section. The top signal is measured after the RFQ linac, and the bottom signal is measured before the Alvarez linac.

peak current was 250 μA with the pulse width of about 50 μs. The pedestal offset before and after the beam pulse is the holding offset of the sample hold circuit. The high frequency noise before and after the beam signals are the thyratron noises of the PFN for the klystron power supply. Because the time constant of the droop is much longer than the pulse width, no droop is seen in the measured pulse shape. The rise time of the pulsed beam was measured to be 4 μs without any rise time corruption caused by the monitoring system.

7. CONCLUSIONS

We developed a beam current monitor of the current transformer type. The adjustable input impedance of the current-to-voltage converter enables the beam current measurement at the long pulse and the low current. The offset canceling circuit made the fluctuation of the offset zero. The frequency range of the monitor is from 30 Hz to 1 MHz, and the wide range current response from 30 μA to 10 mA was realized.

In the beam test, the pulsed beam at 250 μA and with the pulse width of 50 μs, was measured without droop and rise time corruption. Although the low frequency noise was much reduced by the offset canceling circuit, the magnetic shielding of the pickup coil may be needed for the precise measurement.

REFERENCES

(1) Ryuji Yamada, "New Magnetic Pickup Prove for Charged Particle Beams", *Japan. J. Appl. Phys.*, Vol.**1**, No.2, 92-100 (1962).

(2) John M. Anderson, "Wide Frequency Range Current Transformers", *Rev. Sci. Inst.*, Vol.**42**, No.7, 915-926 (1971).

(3) F. R. Gallegos, L. J. Morrison, and A. A. Browman, "The Development of a Current Monitor System for Measuring Pulsed-Beam Current Over a Wide Dynamic Range", *IEEE Trans. Nucl. Sci.*, Vol.**NS-32**, No.5, 1959-1961, October (1985).

(4) R. L. Witkover, E. Zitvogel and V. Castillo, "Beam Current Monitoring in the AGS Booster and its Transfer Lines", *Proc. of the 1991 IEEE Particle Accelerator Conf.*, pp. 1267-1269.

(5) L. P. Huelsman, "Theory and Design of Active RC Circuits", McGraw-Hill Inc., New York (1968).

(6) J. G. Graeme, G. E. Tobey, L. P. Huelsman, "Operational Amplifier Design and Applications", Burr-Broun Corporation (1971).